

See discussions, stats, and author profiles for this publication at: <https://www.researchgate.net/publication/350154418>

A REGIONAL PERFORMANCE-BASED SEISMIC ASSESSMENT TOOLBOX FOR NONDUCTILE CONCRETE BUILDINGS

Conference Paper · September 2020

CITATIONS

0

READS

11

5 authors, including:



[Peng-Yu Chen](#)

University of California, Los Angeles

2 PUBLICATIONS 0 CITATIONS

[SEE PROFILE](#)



[Shuochuan Meng](#)

University of California, Los Angeles

1 PUBLICATION 0 CITATIONS

[SEE PROFILE](#)



[Abdoulreza Ghotbi](#)

University of California, Los Angeles

30 PUBLICATIONS 464 CITATIONS

[SEE PROFILE](#)



[Ertugrul Taciroglu](#)

University of California, Los Angeles

209 PUBLICATIONS 1,941 CITATIONS

[SEE PROFILE](#)

Some of the authors of this publication are also working on these related projects:



Reduced order modeling of soil structure interaction problems [View project](#)



Classifying Seismic-Vulnerable Buildings Based on 3D Models for City Resilience. [View project](#)



A REGIONAL PERFORMANCE-BASED SEISMIC ASSESSMENT TOOLBOX FOR NONDUCTILE CONCRETE BUILDINGS

P.Y. Chen⁽¹⁾, S. Meng⁽²⁾, A. Ghotbi⁽³⁾, A. Sextos⁽⁴⁾, and E. Taciroglu⁽⁵⁾

⁽¹⁾ Graduate Researcher, University of California Los Angeles, sam75782008@ucla.edu

⁽²⁾ Graduate Researcher, University of California Los Angeles, vessel@ucla.edu

⁽³⁾ Project Engineer, Englekirk Structural Engineers, civil_ghotbi40@yahoo.com

⁽⁴⁾ Professor, University of Bristol, a.sextos@bristol.ac.uk

⁽⁵⁾ Professor, University of California Los Angeles, etacir@ucla.edu

Abstract

Recent advances in data analytics, machine learning and cloud-based distributed computing are providing unprecedented opportunities for seismic risk assessment studies at regional (e.g., city) scales. Such capabilities are bound to advance the state-of-the-art in hazard-driven urban planning and actuarial studies as well as post-disaster recovery. Prior regional hazard classification studies on the west-coast cities in the US have revealed several types of buildings that are particularly vulnerable to seismic hazards. Chief among them are the so-called nonductile reinforced concrete buildings (NDRCBs), which bear life-safety risks. There have been numerous efforts on developing detailed inventories of NDRCBs in California, and the circa-2015 count of such buildings stand at approximately 40,000 NDRCBs. These identification studies were followed by a seismic ordinance that requires structure-specific analysis of the identified buildings to choose between demolition and retrofitting.

The present study aims to devise and verify the key ingredient of a toolbox, which is under development, that integrates various existing workflows with new ones in order to achieve semi-automated and performance-based seismic risk assessment of California's NDRCBs. The proposed toolbox will output structure- and site-specific collapse fragility functions. To that end, the toolbox will feature an automated "design procedure" that generates an accurate numerical model of a given NDRCB based on internet-harvested metadata such as the number of floors, floor heights, floor areas, and occupancy type, using the 1967 Uniform Building Code (UBC). This manuscript presents the said automated design procedure, together with its verification against previously evaluated NDRCB models developed from structural drawings. Once fully developed and adequately verified/validated, the proposed toolbox can be applied to a regional inventory of buildings and can become a resource for insurance companies, building owners (or potential buyers), as well as state/city planners. The modules of the developed toolbox can also be replaced or revised to handle other hazards (e.g., hurricanes) and asset types.

Keywords: Regional Seismic Assessment, Nonductile Reinforced Concrete Buildings, PBEE, Collapse Fragility.



1. Introduction

The seismic vulnerability of NDRCBs has been explored after a number of major earthquakes in the past (Fig.1). The poor performance of this building type is primarily due to lack of confinement of the concrete cores of beams, columns, joints, and walls, which causes brittle—as opposed to the desirable *ductile*—behavior in structural components and even collapse. NDRCB was a prevalent construction type in the western U.S. prior to the development and enforcement of modern building codes in the mid-1970s. Many efforts have been undertaken to identify and generate a reliable database of this type of collapse-prone buildings. The California Seismic Safety Commission estimates the number of state's NDRCBs as 40,000 [1]. Concrete Coalition, a network of engineer volunteers, identified 20,000 to 23,000 NDRCBs in California including comprising residential, commercial, and public (e.g., school) buildings [2, 3]. Anagnos et al. [4] documented an inventory of approximately 1,600 NDRCBs in the city of Los Angeles using various databases, and open-access online resources, which provides their geographic distribution and general characteristics. The City of Los Angeles announced a seismic ordinance that requires the mandatory retrofit of soft-story buildings and NDRCBs in 2015. At the present time, the Department of Building and Safety of Los Angeles has sent out the order for 1,376 owners and 1,113 buildings are pending for compliance of the assessment [5].

Due to the nominal need for region-scale seismic risk assessment of NDRCBs throughout the world, the ultimate aim of the present research effort is to integrate a variety of Performance-Based Earthquake Engineering (PBEE) tools into a single workflow, which includes generating structure-specific analysis models, characterizing site-specific hazards, and performing the requisite analyses for evaluating the damage/loss probabilities for different groups of users ranging from professional engineers to stakeholders. The ultimate outcomes of the toolbox will be the engineering demand parameters (EDPs)—such as inter story-drifts and floor accelerations—and the collapse fragility functions per each NDRCB at regional scales.

These regional-scale analyses will feature two types/tiers of models—namely, a multi-story concentrated-mass shear (MCS), and a refined frame model. The former is a simplified model amenable for large (e.g., city-scale) computations, while the latter offers a state-of-the-art detailed assessment requiring both more computational resources and metadata. A parametric MCS model has been recently implemented and became available in the regional workflow devised by the Natural Hazards Engineering Research Infrastructure (NHERI) Computational Modeling and Simulation Center (SimCenter) [6], and the refined model is devised here, which is inspired by previous studies on assessing the collapse risk of buildings [7, 8, 9]. In the remainder of the manuscript, derivation of the refined model and its verification against models devised from structural drawings are presented, together with comparisons of its fragility predictions against the current SimCenter MCS model.

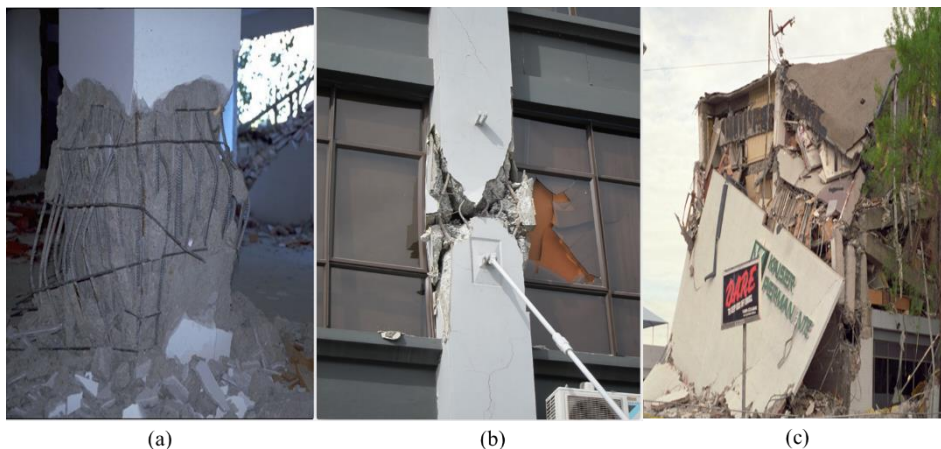


Figure 1. (a) Axial failure at lap splice in a column of a 6-story RC frame [10], (b) shear failure in a column of a 4-story RC frame and core-walls structure [10], and (c) sideway collapse of a 5-story RC structure [11].



2. NDRCBs

Two types of models for NDRCBs are considered in the present study. Both model types are generated based on basic building metadata—namely, floor heights, number of floors, floor areas, and occupancy type. The first model type is the MCS model described earlier, which is simply generated by feeding the aforementioned metadata into an existing NHERI SimCenter workflow [6]. The second model type (henceforth referred to as the *refined model*) is devised in the present study, which makes use of a heuristic algorithm based on 1967 Uniform Building Code. The following sections describe the details of these two model types and how response analyses are carried out using them.

2.1 Multi-story Concentrated-mass Shear Model

In order to evaluate the seismic performance for either a single building or a city-scale number of buildings, the toolbox should be able to generate numerical models through limited data and analyze them in an affordable time. To achieve that, a multi-degree of freedom lumped-mass model, named the multi-story concentrated-mass shear (MCS) model [12,13], is integrated into the proposed toolbox.

In [12], the inter-story mechanical behavior of the MCS can be described by the trilinear backbone curve and three different hysteretic models. The trilinear curve shown in Fig.2 is proposed by HAZUS [14] and can be computed by 5 parameters: k_0 (the initial stiffness), v_y (the shear yielding strength), η (the hardening ratio), α (the ratio of peak strength to yield strength), and Δ_c (the inter-story drift of the complete damage state). According to the seismic performance data of typical buildings specified in HAZUS (Table 5.5 and Table 5.7), these parameters can be determined based on their structural types, story heights, number of stories, construction time, and floor areas. In order to simulate NDRCBs where shear failure is dominated, the pinching model [15, 16] is chosen as the hysteretic material of MCS to describe the inter-story force-deformation behavior.

The buildings are assumed to be symmetric, and thus only two-dimensional models are analyzed. The system damping ratio is assumed to be 5% for the first and the second modes. All floors are assumed to have the same height, mass, and initial stiffness. Under these simplifying assumptions, the initial inter-story stiffness can be computed through

$$k_0 = \lambda \frac{4\pi^2 m}{T_1^2} \quad (1)$$

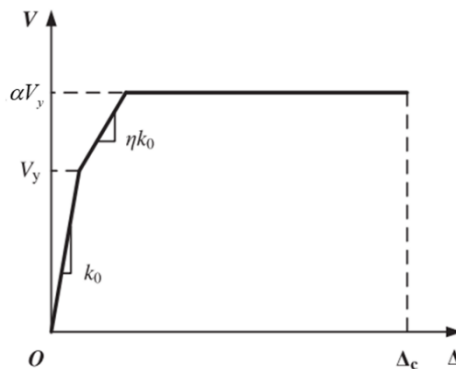


Figure 2. The trilinear inter-story shear force and drift backbone curve (adapted from [13]).

where m is the floor mass, T_1 is the first period obtained from the recommended formula specified in Table 5.5 of HAZUS, and λ is computed as



$$\lambda = \frac{([\phi_1]^T [A] [\phi_1])}{([\phi_1]^T [I] [\phi_1])} \quad (2)$$

Here ϕ_1 is the first mode shape of the building and $[A]$ is a symmetric banded matrix given as,

$$[A] = \begin{bmatrix} 2 & -1 & & & & \\ -1 & 2 & & & & \\ & & \ddots & & & \\ & & & 2 & -1 & \\ & & & -1 & 1 & \end{bmatrix}. \quad (3)$$

The yield strength in shear of each floor is obtained through

$$V_i = V_1 * \left(1 - \frac{i(i-1)}{n(n+1)} \right) \quad (4)$$

$$V_1 = A_y * \alpha_1 * w_{\text{Total}} \quad (5)$$

where V_1 is the base shear capacity, A_y is the yielding spectral acceleration of the building specified in Table 5.7 of HAZUS, α_1 is the fraction of the building weight effective in the push-over mode specified in Table 5.5 of HAZUS, i is the floor number, w_{Total} is the total weight of the building, and n is the number of floors. The ratio of ultimate strength to the yielding strength η in Fig. 2 is then computed as

$$\eta = \frac{A_u - A_y}{D_u - D_y} * \frac{D_y}{A_y} \quad (6)$$

where $\{D_y, A_y\}$ respectively denote the yielding displacement and the yielding spectral acceleration, and $\{D_u, A_u\}$ respectively denote the ultimate displacement and the yielding spectral acceleration. Their values are provided in Table 5.7 of HAZUS.

2.2 The Refined Model

The proposed toolbox aims to provide models with different levels of detail for the different tiers of users. While the MCS can be utilized for rapid post-event assessment, it can neither capture the instant and location of shear failure in columns nor the loss of axial capacity. It is therefore necessary to devise a refined model that can simulate the strength and the stiffness degradation as well as the shear behavior of NDRCBs. However, detailed metadata on NDRCBs at regional scales are limited. Hence, the proposed toolbox introduces an automated design procedure to generate a relatively refined OpenSees model based on the 1967 Uniform Building Code (UBC), which was the primary design guideline document for California's NDRCB stock.

Two types of frame systems (space and perimeter frames, shown in Fig.3) are offered in the toolbox, which are typical [17]. To reduce the computational demand inherent to regional assessment, the considered models are all assumed to be symmetric in two horizontal directions, and any structural irregularities are ignored. In the UBC, lateral force demand depends on base shear (V) computed from $V = CKW$. In this approximation formula, W is the weight of the building, C is the base shear coefficient that determined by Eq. (6)—which, in turn, depends on the period of the structure and shall not be larger than 0.1—, and K is the horizontal force factor, which varies from 0.67 (ductile) to 1.33 ($K = 1$ for nonductile frames). In the proposed approach, W is calculated based on the floor area, the floor weight including dead and live loads, and the number of floors. The dead load is assumed to be 200 psf in order to be consistent with the MCS model. The



live load is assigned based on the occupancy specified in Table 23 of the UBC. The tributary areas of both space and perimeter frame configurations are illustrated in Fig.3, which are used to determine the weight that contributes to lateral forces. C is calculated here based on the structural period that is assumed to be 0.1 times the total number of floors [18]. K is fixed as 1 for all NDRCBs.

$$C = \frac{0.05}{\sqrt[3]{T}} \quad (7)$$

Once the base shear is obtained, the distributed lateral forces can be computed through Eq. (8) to (10) wherein F_r and F_i represent the lateral forces applied at the roof and the i -th floor; h_x , w_x , h_n , and w_n are the height and the floor weight at the x -th floor and roof in respective pairs; D_n is the plan dimension of the vertical lateral force resisting system at the roof.

$$V = F_r + \sum_{i=1}^n F_i \quad (8)$$

$$F_i = 0.004V \left(\frac{h_n}{D_n} \right)^2 \quad (9)$$

$$F_x = \frac{(V - F_r)w_x h_x}{\sum_{i=1}^n w_i h_i} \quad (10)$$

The load combination required by the UBC is utilized to analyze the maximum and the second-largest internal forces for checking the capacity of components of the first floor and the typical floor (2nd and above). The Ultimate Strength Design method and the detailing requirements specified in sec.2615, sec.2616, sec.2617, and sec.2619 in the UBC67 are applied to the archetype structures. Although it is not specified in the UBC67, 2% inter-story drift limitation (Table12.12-1 in ASCE 7-10) is also included in the design procedure to prevent the numerical instability in the early stage of nonlinear time history analysis.

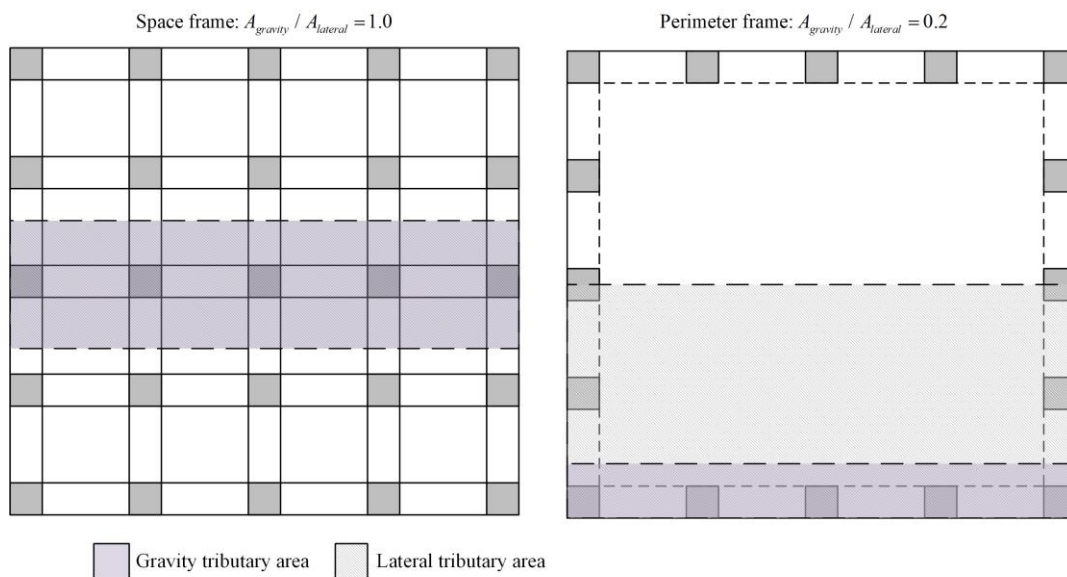


Figure 3. Planview and ratio of gravity to lateral tributary areas of two archetype structures.



Fig.4 delineates the design procedure for the refined model. In order to obtain the demands of components, a preliminary OpenSees model must be devised to perform the static analysis. Six archetypal nonductile RC frames are selected from the study by Liel et al. [9] as initial designs for structures with different heights (i.e., low-, mid-, and high-rise) and types (i.e., perimeter and space frame). With the preliminary model, the observed forces can then be utilized to check the provided capacities of components. If the capacity is insufficient, then the proposed algorithm will iteratively modify the reinforcement details (i.e., numbers and sizes of rebars), and member dimensions (e.g., depth and width). For the drift ratio check, the maximum inter-story drift should not exceed 2%. If the drift ratio limit is violated, only the dimensions of components will be modified then the algorithm will move forward to the next analysis and check. It must be noted that the “refined” model is not the as-built model but only an approximation to it; however, a preliminary validation against a detailed model is provided in the following section.

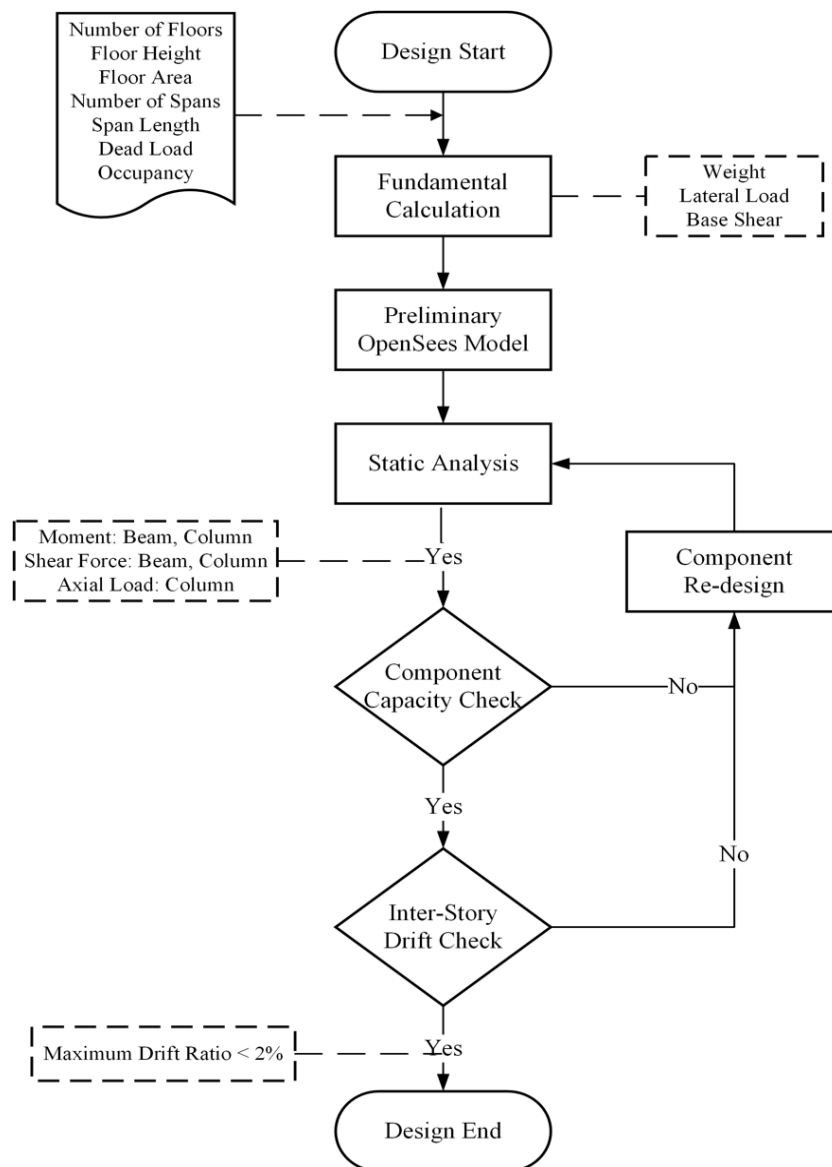


Figure 4. The design procedure of a refined model in the proposed toolbox.



Once the design procedure is completed, the proposed procedure automatically generates an OpenSees model, such as that shown in Fig.5. It must be emphasized here that an elastic beam-column element is used in devising the model, and not a fiber beam-column element, in order to reduce the computational cost. For the same reason, the brittle failure model considered here only captures the shear and axial failure in columns but not the joint-shear failure. Moreover, shear and axial failure modes are not considered in the beam since the UBC67 typically results in a strong-beam weak column.

The concentrated plastic hinge (Fig.5) is used in the proposed model to simulate the strength deterioration [19, 20], and the material model used for defining its response in OpenSees is the Modified Ibarra-Medina-Krawinkler model with the peak-oriented hysteretic response. Six parameters are required to control the monotonic and cyclic behavior—namely, the elastic stiffness K_e , the yielding moment M_y , the ratio of capping to yield moment M_c / M_y , the plastic rotation in post-yielding region θ_p , the post capping rotation θ_{pc} , and the ultimate rotation θ_u , which are determined based on the regression equations calibrated using 255 RC column experiments [8]. Although the plastic hinge does not account for the interaction of axial loads and moments in columns, it is able to capture strain-softening and rebar-buckling effects [21].

In order to simulate the stiffness and strength degradation due to shear failure and the loss of axial capacity, the limit-state material developed by Elwood [22] is implemented in the proposed model. The axial and shear springs are accompanied by rotational springs at both ends of the column, behaviors of which are defined through a limit-state material curve. Shear failure is triggered once the column's total response exceeds the shear limit curve. The shear limit curve consists of shear capacity V_n , degrading slope K_{deg} , and residual shear strength V_{res} , which are defined in [22] based on experimental data. Similarly, once the response exceeds the axial limit curve, axial failure will be triggered. Axial failure tends to occur when the shear strength degrades to approximately zero. The details of calculations can be found in [23].

2.3 Nonlinear static analysis

To verify that the proposed model is capable of capturing the critical behavior of NDRCBs, a well-known nonductile RC building—namely, the Van Nuys Hotel, which was designed in 1965 per the 1964 Los Angeles Building Code—is chosen. The hotel has a 9,450 ft² floor area and 3 by 8 bays. The first story is 13.5 ft high and the rest of the floors are 8.5 ft high. The south side of the building forms the lateral force-resisting system, which is represented as a two-dimensional OpenSees model that is created using the procedure described above. Numerous comprehensive seismic assessment studies on the Van Nuys Hotel had been carried out previously [24–25], and the pushover curve provided in [25] is compared with that obtained using the procedure devised in the present study.

Table 1 summarizes the differences in the assumptions used in [25] and the proposed model. The components are simulated using fiber-hinge beam-column line elements in [25] but only the elastic beam-column element and the concentrated plastic hinge are utilized in the proposed model. For the simulation of column shear failure, a shear-force-versus-shear-distortion model [26] that is independent of the loading history and drift demand is utilized in the reference model; but the column shear failure model that defines shear strength as a function of inter-story drift [22] is applied in the proposed model.

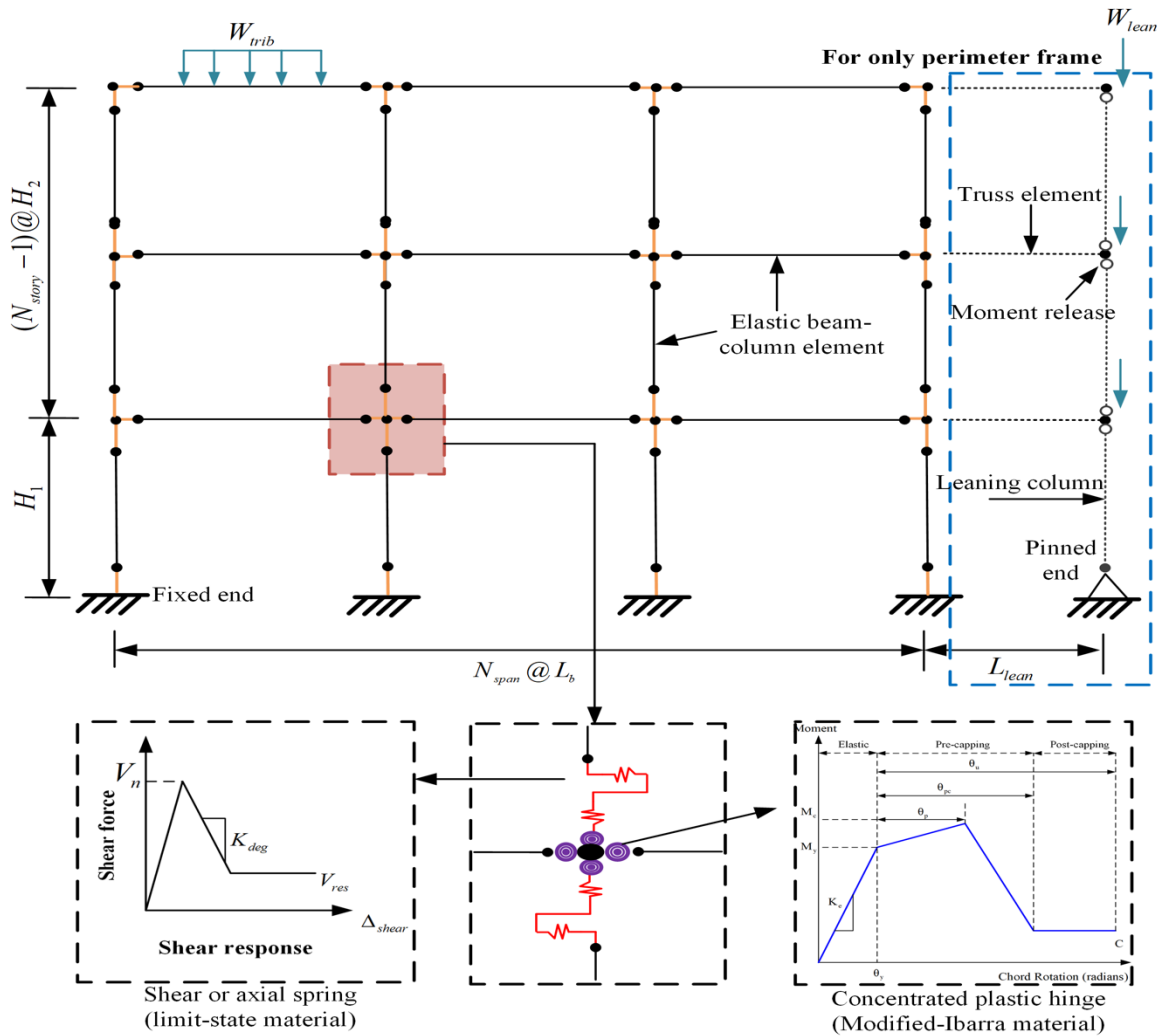


Figure 5. Frame model.

Table 1. Comparison of assumptions

	Krawinkler [25]	Proposed
f'_c Beam / f'_c Column	4 ksi / 5 ksi	4 ksi / 4 ksi
f_y Beam / f_y Column	50 ksi / 75 ksi	40 ksi / 60 ksi
Plastic hinge	Force-based fiber element	Concentrated plastic hinge
Shear failure model	Shear force and shear distortion model	Limit state material and limit curve
Loss of axialload capacity	Not included	Included
P-Delta effect	Not included	Included
Gravity load	Not included	Included

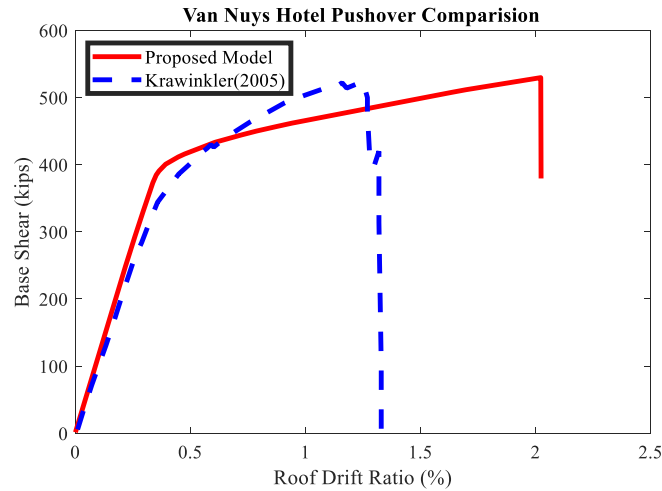


Figure 6. Comparison of nonlinear pushover curves.

The pushover loading pattern implemented in the proposed procedure is calculated based on the equivalent lateral force specified in ASCE 7-10 whereas the lateral load distribution recommended in FEMA 356 was utilized in [25]. As shown in Fig 6, the initial stiffness and the maximum base shears of both models are similar but the ultimate drift ratios are different. The reason for this discrepancy is due to the consideration of gravity loads in the proposed model, which causes higher axial loads, which, in turn, increases the shear capacities of the columns per the shear limit state material model provided in [22]. As mentioned above, the proposed model generation procedure features only two types of sections (i.e., first floor and typical floor), which may be conservative compared to the as-built model. However, the pushover curves shown in Fig.6 suggest that the proposed model generation procedure can accurately capture the dominant (i.e., flexural-shear) failure mode .

3. Collapse Evaluation

In order to assess the collapse probability of NDRCBs, Incremental Dynamic Analyses (IDA) [27] carried out. In IDA, nonlinear time-history analyses are repeated for a single model subjected to a large set of ground motions, so the probability distribution of a specific damage state (e.g., collapse) as a function of intensity measure (IM) can be produced (i.e., fragility curves). In this study, the far-field record set of 44 (22 pairs) ground motions specified in FEMA P695 [28] are selected for the IDAs. The magnitude of the selected records varies from M6.5 to M7.6 with an average of M7.0, and the peak ground acceleration varies from 0.21g to 0.82g with an average of 0.43g.

During IDA, the median spectral acceleration of the record set is scaled from 0.2g to 5.0g at an increment of 0.2g to extract the empirical collapse data. Collapse is taken as the point at which dynamic instability occurs or a certain drift limit is exceeded. In the presented IDA results, the drift threshold of the complete damage state is assumed to be 5% based on Table 5.9 in HAZUS.

To develop the collapse fragilities, the median collapse intensity and the dispersion of the lognormal distribution are computed through the maximum likelihood approach. The probability of collapse for a few levels of IM can be obtained through

$$P(C) = \varphi\left(\frac{\ln(IM_i / \theta)}{\beta}\right) \quad (11)$$

If the analysis is carried out for n_j GMs, then the probability of z_j collapse out of n_j GMs can be derived using a binomial distribution as shown in



$$P(z_j \text{ collapse out of } n_j \text{ GMs}) = \binom{n_j}{z_j} (P(C))^{z_j} (P(NC))^{n_j - z_j} \quad (12)$$

If the analyses are done for multiple levels of IM, it is fair to assume that each level is independent of the other. Doing so, the binormal probability for all levels of IM is the product of each IM level, that is

$$\text{Likelihood} = \prod_{j=1}^m \binom{n_j}{z_j} (P(C))^{z_j} (P(NC))^{n_j - z_j} \quad (13)$$

Then, the likelihood function should be maximized as in

$$\{\hat{\theta}, \hat{\beta}\} = \arg \max_{(\theta, \beta)} \sum_{j=1}^m \left\{ \ln \binom{n_j}{z_j} + z_j \ln \varphi\left(\frac{\ln(IM_i / \theta)}{\beta}\right) + (n_j - z_j) \ln \left(1 - \varphi\left(\frac{\ln(IM_i / \theta)}{\beta}\right)\right) \right\} \quad (14)$$

where $\hat{\theta}, \hat{\beta}$, which are the median and the standard deviation values of the collapse fragility function.

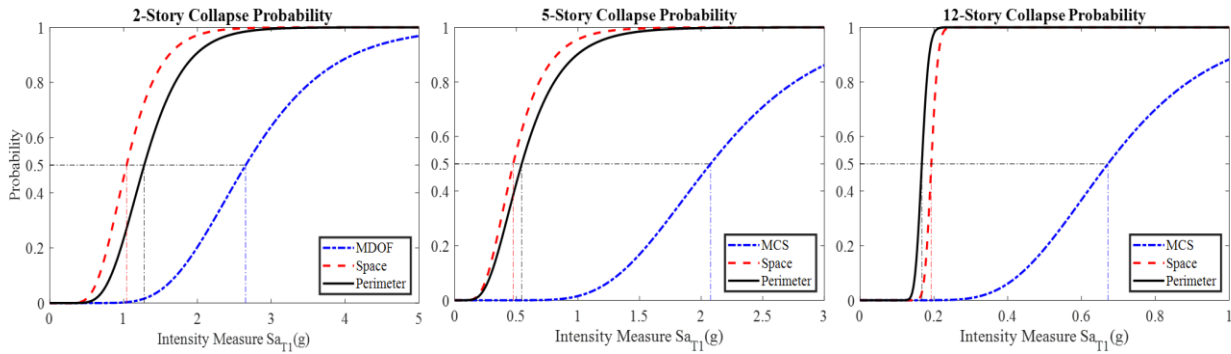


Figure 7. Comparison of collapse fragilities.

Fig.7 displays the fragilities of three representative—namely, low-rise, mid-rise, and high-rise—buildings obtained using MCS, perimeter frame, and space frame models. All buildings considered here have a floor area of 5,468 m², and story heights of 3.21 m, which are average values obtained for an extensive NDRCB database [29].

Table 2. Median collapse intensity (g).

Number of stories	MCS	Perimeter frame	Space frame
2	2.7	1.3	1.0
5	2.1	0.54	0.48
12	0.67	0.17	0.19

For all three model types, the collapse probabilities increase with height, as summarized in Table 2. On the other hand, the MCS model overestimates the collapse safety, because the hysteretic model it features cannot mimic strength deterioration. The perimeter frame has a higher median collapse intensity in low-rise and mid-rise buildings than the space frame, because the lateral force dominates the design procedure. In contrast, gravity loads are more important during the design of low-rise and mid-rise space frames. For the high-rise building, the $P-\Delta$ effects are more significant in the perimeter frame, which results in a lower median collapse intensity.



4. Conclusions and Future Studies

This paper summarizes the authors' preliminary efforts in developing a toolbox for regional seismic assessment for nonductile reinforcement concrete buildings (NDRCBs). The proposed toolbox utilizes basic metadata from buildings to generate numerical models that can capture collapse behavior. This is achieved by devising a design flowchart that follows the 1967 Uniform Building Code and uses the basic metadata (floor heights, number of floors, floor areas, occupancy type, etc.). This proposed procedure is successfully verified using a pushover curve obtained for a representative NDRCB (i.e., Van Nuys Building) that was extensively examined in prior studies [e.g., 25].

The proposed toolbox includes IDA to evaluate the collapse fragilities of NDRCBs. Although only three representative model buildings are examined in this paper, the toolbox can be easily scaled (through the use of parallel/cloud computing resources) and be applied to large building inventories [see, for example, 29]. The toolbox is capable of considering site-specific ground motions. In the presented fragilities, the collapse performance worsens with height, and $P-\Delta$ effects become significant in the high-rise perimeter frame building type.

Predictions of the proposed procedure are also compared with those made using a parametric multi-story concentrated-mass shear (MCS) model, which recently became available in the regional workflow devised by the Natural Hazards Engineering Research Infrastructure (NHERI) Computational Modeling and Simulation Center (SimCenter) [6]. These comparisons indicate that these MCS models underestimate the collapse fragilities, because the hysteretic material model used in their construction cannot capture strength deterioration. Moreover, MCS model considers only sideways collapse, whereas the proposed model can capture collapse due to loss of axial capacity, including effects.

5. References

- [1] Governor's Office of Emergency Services (OES), 2004. State of California Multi Hazard Mitigation Plan, available at <https://www.caloes.ca.gov/home>.
- [2] Comartin CD, Anagnos T, Faison H, Greene M, Moehle JP. The Concrete Coalition: Building a network to address nonductile concrete buildings. In *Proceedings, 14th World Conference on Earthquake Engineering* 2008 Oct.
- [3] Comartin C, Bonowitz D, Greene M, McCormick D, May P, Seymour E. The Concrete Coalition and the California Inventory Project: An Estimate of the Number of Pre-1980 Concrete Buildings in the State. September, Oakland, CA: The Earthquake Engineering Research Institute. 2011 Sep.
- [4] Anagnos T, Comerio MC, Goulet C, Na H, Steele J, Stewart JP. Los Angeles inventory of nonductile concrete buildings for analysis of seismic collapse risk hazards. In *Proceedings of the 14th World Conference on Earthquake Engineering* 2008 Oct 12.
- [5] Los Angeles Department of Building and Safety (LADBS), 2019. Non-ductile Concrete Retrofit Program, available at <http://ladbs.org/services/core-services/plan-check-permit/plan-check-permit-special-assistance/mandatory-retrofit-programs/non-ductile-concrete-retrofit-program>.
- [6] Elhaddad, W., McKenna, F., Rynge, M., Lowe, B.J., Wang, C., & Zsarnoczay, A. (2019). NHERI-SimCenter/WorkflowRegionalEarthquake: rWHALE (Version v1.1.0), available at <https://simcenter.designsafe-ci.org/research-tools/regional-workflow/>.
- [7] Ibarra LF, Medina RA, Krawinkler H. Hysteretic models that incorporate strength and stiffness deterioration. *Earthquake engineering & structural dynamics*. 2005 Oct;34(12):1489-511.
- [8] Haselton CB, Goulet CA, Mitrani-Reiser J, Beck JL, Deierlein GG, Porter KA, Stewart JP, Taciroglu E. An assessment to benchmark the seismic performance of a code-conforming reinforced-concrete moment-frame building, *PEER Report 2007/12*, Pacific Earthquake Engineering Research Center. University of California, Berkeley, United States. 2008.



- [9] Liel AB, Haselton CB, Deierlein GG. Seismic collapse safety of reinforced concrete buildings. II: Comparative assessment of nonductile and ductile moment frames. *Journal of Structural Engineering*. 2011 Apr 1; **137**(4):492-502.
- [10] Earthquake Engineering Research Institute (EERI), 2013. Online Database of Concrete Buildings Damaged in Earthquakes, available at <http://db.concretecoalition.org/>.
- [11] U.S. Geological Survey (USGS), 2006. Damage Photos, USGS Photographic Library, available at <https://www.usgs.gov/>.
- [12] Lu X, Han B, Hori M, Xiong C, Xu Z. A coarse-grained parallel approach for seismic damage simulations of urban areas based on refined models and GPU/CPU cooperative computing. *Advances in Engineering Software*. 2014 Apr 1; **70**:90-103.
- [13] Zeng X, Xu Z, Lu X. Regional Seismic Damage Simulation of Buildings: A Case Study of the Tsinghua Campus in China. *In Computing in Civil Engineering 2015* 2003 Jan (pp. 507-514).
- [14] Federal Emergency Management Agency (FEMA). 2012. Multi-hazard loss estimation methodology: earthquake model, HAZUS – MH2.1 technical manual. Washington, D.C.
- [15] Hidalgo PA, Jordan RM, Martinez MP. An analytical model to predict the inelastic seismic behavior of shear-wall, reinforced concrete structures. *Engineering Structures*. 2002 Jan 1; **24**(1):85-98.
- [16] Voon KC. In-plane seismic design of concrete masonry structures (Doctoral dissertation, ResearchSpace@ Auckland).
- [17] Liel AB, Deierlein GG. Using collapse risk assessments to inform seismic safety policy for older concrete buildings. *Earthquake Spectra*. 2012 Nov; **28**(4):1495-521.
- [18] American Society of Civil Engineers. (2013). Minimum Design Loads for Buildings and Other Structures (ASCE/SEI 7-10). American Society of Civil Engineers.
- [19] Ibarra LF, Krawinkler H. Global collapse of frame structures under seismic excitations. *Rep. no. TB 152*, The John A. Blume Earthquake Engineering Center.
- [20] Lignos DG, Krawinkler H. Development and utilization of structural component databases for performance-based earthquake engineering. *Journal of Structural Engineering*. 2013 Aug 1; **139**(8):1382-94.
- [21] Lynch KP, Rowe KL, Liel AB. Seismic performance of reinforced concrete frame buildings in Southern California. *Earthquake Spectra*. 2011 May; **27**(2):399-418.
- [22] Elwood KJ, Moehle JP. Shake table tests and analytical studies on the gravity load collapse of reinforced concrete frames, *PEER report 2003/01*. University of California, Berkeley. 2003.
- [23] Elwood KJ, Moehle JP. Drift capacity of reinforced concrete columns with light transverse reinforcement. *Earthquake Spectra*. 2005 Feb; **21**(1):71-89.
- [24] Somerville P, Collins N. Ground motion time histories for the Van Nuys building. *PEER Methodology Testbeds Project*. 2002 Mar 7.
- [25] Krawinkler H. Van Nuys hotel building testbed report: exercising seismic performance assessment. Pacific Earthquake Engineering Research Center. University of California at Berkeley, Berkeley, California. 2005.
- [26] Kowalsky MJ, Priestley MN. Improved analytical model for shear strength of circular reinforced concrete columns in seismic regions. *Structural Journal*. 2000 May 1; **97**(3):388-96.
- [27] Vamvatsikos D, Cornell CA (2002): Incremental dynamic analysis. *Earthquake Engineering & Structural Dynamics*, **31** (3), 491-514.
- [28] Federal Emergency Management Agency (FEMA), 2009. Quantification of Building Seismic Performance Factors, FEMA P695, Washington, D.C.
- [29] Older concrete buildings in Los Angeles, (2014). Los Angeles Times. Retrieved from <http://graphics.latimes.com/la-concrete-buildings/>